

Synthetic Report

of research projects for young research teams - *PN-II-RU-TE-2011-3-0124*
(October 2011 – September 2014)

1. Excited State Relaxation Processes for 5- and 6-Benzyluracil Molecular Systems

The benzyluracil (BU) can be considered as a model system for the photo-crosslink reaction [1] in biological systems. It contains a benzene ring (which replaces the aromatic part of phenylalanine) and a uracil base which are covalently connected through a methylene bridge. The first and second singlet excited state of the 5- and 6-benzyluracil (5BU and 6BU) as well as its electronic excited state relaxation pathways were theoretically investigated using multi-reference Hartree-Fock (state-averaged CASSCF) and electron correlation methods (CASPT2, MRCI and EOM-CCSD). The vertical excitation energies, equilibrium geometries of low-lying excited-states as well as the conical intersection (CI) points between different potential energy surfaces (PES) were characterized in terms of molecular geometry, natural population and bond order analysis.

The geometry optimization calculations for BU systems have been performed at the state-averaged CASSCF theory level using the Molpro computational chemistry program package [2]. In this case Dunning's double ζ + polarization (DZP) basis set [3] was considered and no symmetry restrictions were considered for the molecular geometry. According to Matsika's [4] and Epifanovsky's [5] studies, if we neglect Rydberg states, the lowest excited states of the uracil fragment originate from excitations of the valence p and lone pair n_o orbitals. Eight p and two n_o lone pair orbitals, from the two oxygen atoms, are located on the uracil part of the molecule, thus an appropriate active space in CASSCF should include these 10 orbitals. On the other side of the molecule (the benzene fragment), there are at least six p orbitals [6], which should be included in the same active space. Therefore, in order to include these effects in the 5BU excitation scheme, the correct active space for the 5BU would be (20,16), the nomenclature (n,m) denoting here an active space of n electrons and m orbitals. In order to take into account the effect of electron correlations (static and dynamic) for the vertical excitation energies evaluation, we have performed further calculations using higher-level methods: (i) multireference configuration interaction (MRCI) [7] with and without Davidson (D) correction [8], (ii) multi state second-order multireference perturbation theory (MS-CASPT2) [9], and (iii) equation-of-motion coupled-cluster theory for excited states (EOM-CCSD) [10-12].

The vertical excitation energies up to the second excited level calculated using different theoretical methods are presented in Table 1. The S_1 vertical excitation energy of 5BU and 6BU systems has the same amount of energy as the isolated fragments, meaning that the S_1 excitation could not be localized only at one of the 5BU or 6BU molecular fragments. This is confirmed by the fact that the dominant reference coefficients of different Slater determinants corresponding to one electron excitation for S_1 states show both uracil – uracil and benzene - benzene transitions. The energies of the S_2 state for both 5BU and 6BU cases are closer to that of the uracil rather than to that of benzene, therefore exhibiting strong uracil character. For the $S_0 - S_1$ transitions we obtained small enough oscillator strengths. This is because we only have a mixture of two pure uracil – uracil and benzene – benzene excitations. For the $S_0 - S_2$ transitions this picture is totally different. In contrast to our expectations, based on the small

oscillator strength values in individual cases of the uracil and benzene, here we found large oscillator strength which can be explained with the charge transfer effect from the uracil to the benzene fragment.

Table 1. Vertical excitation energies (in eV-s) for the two lowest excited states of 5BU and 6BU molecular systems.

Metod	SA-MCSCF	MR-CASPT2	MRCI	MRCI-D	EOM-CCSD	LT-DF-LCC2	TDDFT (B3LYP)	TDDFT (M06-2X)
5BU								
S_1	4.85	4.93	5.08	5.11	5.13	4.94	4.82	5.16
S_2	7.92	6.28	7.12	6.90	5.44	5.07	5.23	5.49
6BU								
S_1	4.84	5.23	5.38	5.37	5.19	4.89	4.72	
S_2	7.90	6.22	6.32	6.30	5.42	5.15	4.91	

It is found that the three unveiled conical intersections could play a crucial role in the 5BU and 6BU decay pathways: as for the single isolated fragments – benzene and uracil – they represent ultrafast non-radiative decay channels leading to lower energy electronic states. As regards the electronic excited state relaxation we have drawn a global picture with different relaxation pathways defined by local minima and conical intersection points on the PESs. The most likely pathway that the molecule can

follow when the excitation leads to the S_2 excited state is the vibrational decay to the $R_e^{U1}(S_2)$ geometry, a process which only involves the uracil ring, then evolving through the $R_{CI}^{U1}(S_1S_2)$ conical intersection to the S_1 PES and relaxing, vibrationally, to the $R_e^{U1}(S_1)$ geometry. Finally the system could energetically reach the $R_{CI}^{U1}(S_0S_1)$ conical intersection geometry leading the electronic state of the molecule to the minima in the ground state initial geometry or directly via radiation decay from $R_e^{U1}(S_1)$ to $R_e(S_0)$. Other possible pathways via the benzene branch start from the S_2 state and reach the S_1 state following the $S_2 \rightarrow R_{CI}^{B1}(S_1S_2)$ (or $R_{CI}^{B2}(S_1S_2)$) $\rightarrow R_e^B(S_1)$ radiationless decays. Eventually the non-radiative $R_e^B(S_1) \rightarrow R_{CI}^B(S_0S_1) \rightarrow R_e(S_0)$ relaxations or the corresponding direct radiative transitions can take the molecule to the S_0 state.

Beside the small deviations in the corresponding energy values, the main difference in the excited state relaxation behavior between the 5BU and 6BU systems is that we could not find any conical intersection points between the S_1 and S_0 PESs only just an avoided crossing and the relaxation process from S_1 and S_0 is realized through direct radiative transitions.

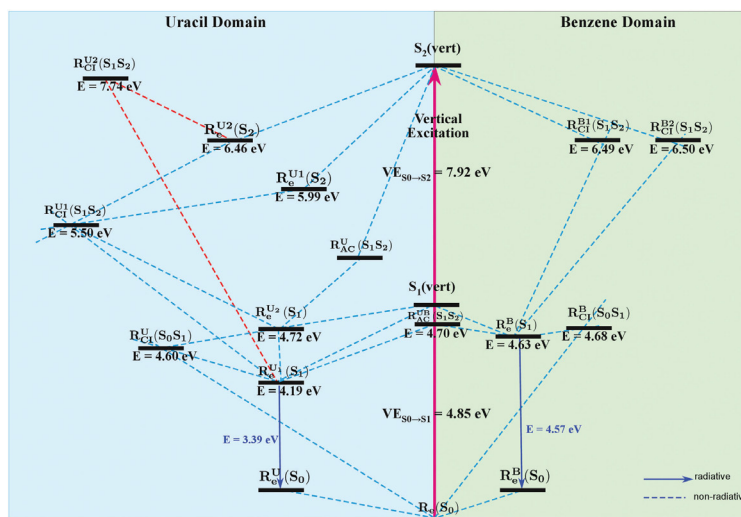


Figure 1. The global energy diagram of different local minima and conical intersection points on the PES for different excited state levels, obtained using the (20,14) active space CASSCF method.

2. Modeling laser induced molecule excitation using real-time time-dependent density functional theory: Application to 5- and 6-benzyluracil

Using real-time propagation theory instead of linear response one can include nonlinear effects and thus stronger laser field can be applied; on the other hand the framework can directly reveal information about the ultrafast dynamics of electrons and ions during the excitation time. The fully propagated real time-dependent density functional theory method [13] has been applied to study the laser–molecule interaction in 5BU and 6BU. The molecular geometry optimization and the time-dependent electronic dynamics propagation were carried out using the M11-L [14] local meta-NGA (non-separable gradient approximations) exchange-correlation functional together with the def2-TZVP basis set [15] implemented in the Molpro program package [2]. Different laser field parameters like direction, strength, and wavelength have been varied in order to estimate the conditions for an efficient excitation of the molecules. The basic laser field parameters were set as: 254 nm for the laser wavelength, $2.24 \cdot 10^{12}$ W/cm² peak intensity. The total propagation time was considered ≈ 23 fs with the time-step of 0.0048 fs. We limit on this time scale in order to keep the conditions for the rigid-body approximation assumed in the case of our molecular systems. The laser field pulse envelope has set in the *trap* form which grows from zero in one field oscillation, stays constant for n periods (in our case $n = 30$) and then decays to zero in one period. A first important finding is that there are significant differences in the case of the efficiency of the laser field absorption applied along the three principal axes of the molecules. 5BU can be easily excited if one applies the laser field along the Y or Z axes, while 6BU could efficiently absorb only if the field is applied along the Z axis. The absorption efficiency can be increased if the polarization of the laser field is not set along one of the principal axes, but through the combination of different vector directions. Accordingly, for 5BU we have obtained the highest excitation efficiency if the field is oriented along the YZ direction, while 6BU gives the highest yield of absorption for the -YZ direction, which is perpendicular on the previous direction. This fact clearly demonstrates the necessity of the molecular alignment before the molecular system is being excited by a laser field. On the other hand, larger charge transfer effect was obtained for the 6BU case than that of 5BU when the laser field polarization is set along the Z axis. Choosing four different wavelengths (240 nm, 254 nm, 270 nm and 290 nm) for the laser pulse a selective behavior for the molecular excitation was observed. Similarly with the theoretical UV spectra obtained using the TDDFT theory, the excitation wavelength of 290 nm is not able to produce significant changes in the electronic structure of the molecules. However, the wavelength of 270 nm could selectively excite only the 5BU molecule against the 6BU and only in the Z direction, the excitation along the Y axis having a very small absorption rate. For lower wavelengths values the selectivity between 5BU and 6BU cases vanish and we obtain a relatively complex picture of one-electron orbital transitions between occupied and virtual orbitals for both molecular cases. Considering different peak intensities of the laser field ($1.40 \cdot 10^{11}$ W/cm², $8.76 \cdot 10^{11}$ W/cm² and $2.24 \cdot 10^{12}$ W/cm²), the molecular response of 5BU and 6BU to the laser excitation also show different pictures. For example, for the highest peak intensity 5BU excitation enters in a saturation regime after 18-19 fs, followed by a decreasing of absorption, while 6BU continuously absorbs photons from the laser field, probably saturation occurs at longer than pulse duration times. On the other hand, the smallest value of the laser field peak intensity is insufficient to have a considerable excitation for the molecules; we have obtained significant laser field absorption only for the last two peak intensity values.

3. Excited State Relaxation Processes for Acetophenone and Benzophenone Systems

Acetophenone ($C_6H_5C(=O)CH_3$, APN) and benzophenone ($C_6H_5C(=O)CH_2C_6H_5$, BPN) systems are the two aromatic ketone molecules with interesting photochemical and spectroscopic properties. Due to the electronic excitation of the π electrons of the carbonyl group or the benzene ring, electron charges can very easily migrate between the carbonyl fragment and the benzene ring and change the electronic structure of the fragments. In general, this π electron conjugation between the aromatic and carbonyl groups could influence the ordering of the $n \rightarrow \pi^*$ and $\pi \rightarrow \pi^*$ states, their photochemical reactivities, and the photo-relaxation or dissociation mechanisms [16-18].

The geometry optimization calculations and the localization of conical intersections between surfaces of the different electronic states of APN and BPN have been performed at the state-averaged CASSCF level of theory using the Molpro computational chemistry program package [2]. For this case the triple ζ def2-TZVP basis set [15] was taken and no symmetry restrictions were considered for the molecular geometry. If we neglect the Rydberg states, the lowest excited states of the APN are originated from the excitations of the valence π and lone pair n_o orbitals. Four π (one from C=O group of the carbonyl fragment and three from the benzene aromatic ring) and one n_o lone pair orbitals, from the oxygen atom, are located on the APN molecule. Thus an appropriate active space in CASSCF should include these five occupied orbitals with ten electrons. On the other hand, describing correctly the valence π excitation of the benzene molecule, according to Robb [6], we should consider at least three virtual orbitals in our active space. So, the final active space for the APN molecule must contain five occupied orbitals, three virtual orbitals and ten electrons. In this way, the active space for the APN would be (10,8). Applying similar consideration for the BPN system its active space would be (16,12) through the addition of the second benzene ring to the APN active space.

The vertical excitation can be more easily understood if one compares the APN and BPN cases with their constituent fragments of the benzene and acetone. Based on this comparison one can observe that the first excited state of both molecules is related to the first excited state of the acetone molecule, while the second excited state can be connected with the first excited state of the benzene. The symmetry of the electronic transition corresponds to the first excited state of the acetone ($n\pi^*$) as well as with the first excited state of the benzene ($\pi\pi^*$). In this way we have analyzed the charge redistribution for different excited states during the vertical excitation. Accordingly, we have found that in the case of the first excited state there is about 0.095e charge migration from the carbonyl fragment to the benzene one in the APN case and (0.086e for the BPN), while for the second excited state we have the opposite effect when about 0.086e charge leaves the benzene ring and appears as an extra charge at the carbonyl fragment (0.057e for the BPN). These different charge migrations for the first and second excited state also demonstrate the nature of the excitation which was concluded before. Analyzing the magnitude of the oscillator strength one was observed that the $S_0 \rightarrow S_1$ transition is a dark state for both molecular systems ($f_{S_0 \rightarrow S_1}^{APN} = 0.0000$ and $f_{S_0 \rightarrow S_1}^{BPN} = 0.0019$) and only the second excited state (S_2) can be reached via the vertical excitation ($f_{S_0 \rightarrow S_2}^{APN} = 0.0091$ and $f_{S_0 \rightarrow S_2}^{BPN} = 0.0063$). It is found that the so-called inter-system crossing point (ISC), where a PES of a singlet electronic state crosses another PES of a triplet electronic state, plays a crucial role in the excited state relaxation processes. Accordingly, we have drawn a global picture with different relaxation pathways defined by local equilibrium minima, conical intersection and inter-system crossing points on the PESs for both APN and

BPN molecular systems. Pathway that the APN molecule can follow when the excitation leads to the S_2 excited state is the vibrational decay to the $R_e^B(S_2)$ geometry, a process which only involves the benzene ring, then evolving through the $R_{CI}^B(S_1S_2)$ conical intersection to the S_1 PES and relaxing, vibrationally, to the $R_e^B(S_1)$ geometry, which is a local minimum. From this local minimum, the system can easily pass over a small energy barrier and reach the global $R_e^C(S_1)$ geometry and can turn back to the ground state via radiation decay from $R_e^B(S_1)$ to $R_e(S_0)$. The only difficulty in going through this relaxation pathway is the relatively high energy position of the $R_{CI}^B(S_1S_2)$ conical intersection from the energy of the $R_e^B(S_2)$ geometry (1.83 eV). As an alternative, the pathways can continue through the $R_{ISC}^B(S_2T_3)$ ISC point by changing its singlet state to the triplet one (the spin-orbit coupling is 0.32 cm^{-1}). This step is followed by a fast relaxation to the first excited triplet state, where the system can again chose between two relaxation directions. Either turns back to the singlet state through the $R_{ISC}^B(S_1T_1)$ ISC point ($SO_{T_1S_1} = 19.8 \text{ cm}^{-1}$) and relaxing, vibrationally, to the $R_e^C(S_1)$ global energy minimum followed by radiation decay from the $R_e^C(S_1)$ to the $R_e(S_0)$ or evolving through the $R_{CI}^B(T_0T_1)$ conical intersection to the T_0 PES and relaxing, vibrationally, to the $R_e^C(T_0)$ geometry followed by direct *phosphorescence decay* to the $R_e(S_0)$ ground state. In conclusion we can state that beyond the pure singlet relaxation pathway the singlet - triplet - singlet relaxation pathway is also feasible. Similar conclusions were drawn also for the BPN molecular system with the difference that while the singlet excited state level of the APN and BPN molecular structures is quite similar, there are significant differences between their triplet states level structure (See Figure 1).

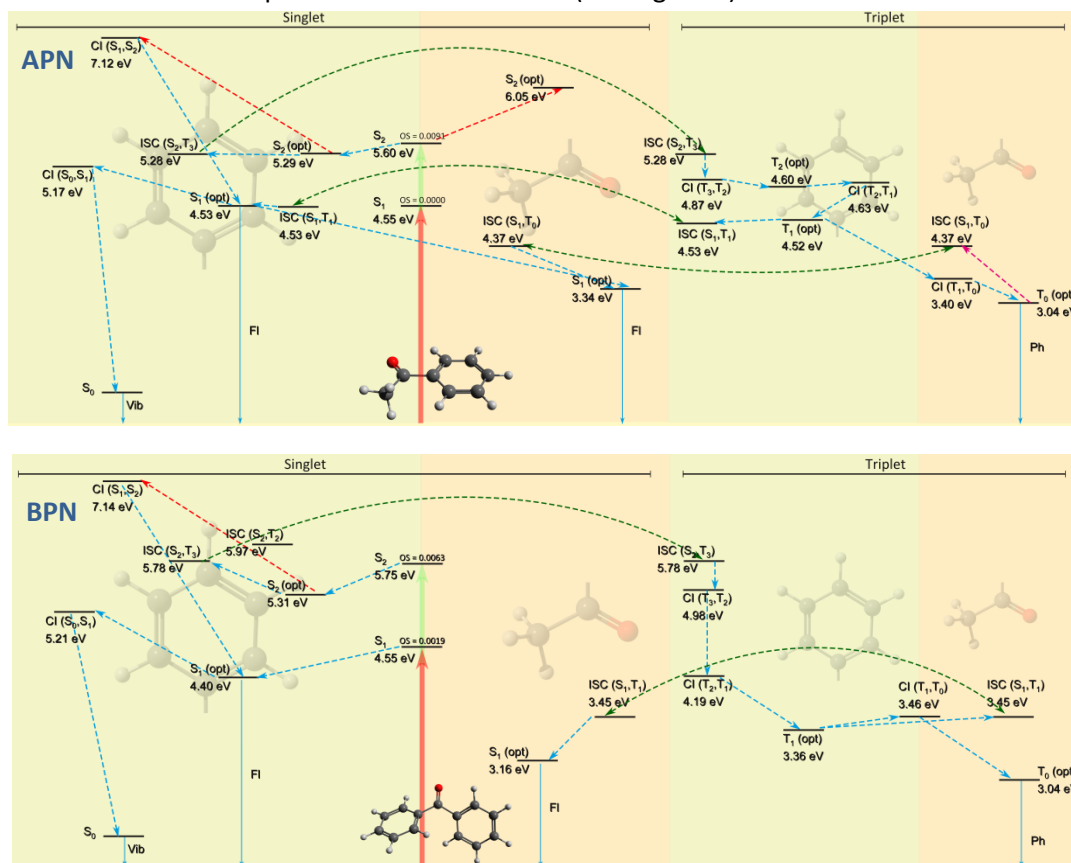


Figure 1. The excited state relaxation schemes for APN and BPN molecular structures.

4. Vertical Excitation and Excited State Equilibrium Geometry Characterization for Octyl-methoxycinnamate and Bis(2-ethylhexyl)-phthalate Molecular Systems.

The molecular geometries of ground and excited states were optimized using the linear response time-dependent density functional theory (TDDFT) method [19] together with M06-2X [20] exchange-correlation functional and def2-TZVP [21] basis set as is implemented in the GAUSSIAN09 program package [22].

In the case of the theoretical UV spectra of the octyl methoxycinnamate we have obtained two relevant absorption windows. The first spectral domain (250 – 295 nm) is characteristic for S_2 vertical excited state having a strong oscillator strength ($f_{S_0 \rightarrow S_2} = 0.9501$) and therefore having also a large full width at half maximum (FWHM) of 25 nm, between 260 – 285 nm. This transition is fully characterized by the HOMO → LUMO transition. The second absorption window is between 180 – 210 nm and includes the $S_5 - S_9$ vertical excited states.

In the case of the theoretical UV spectra of the bis(2-ethylhexyl)-phthalate we have obtained two relevant absorption windows. First is centered on the maximum value of 238 nm with two excited states of $S_1 = 239.27$ nm and, $S_2 = 237.82$ nm, respectively, while the second center is related to the $S_4 = 210.19$ nm excited state value. Analyzing both geometric shape and relaxation of excited states one can conclude that the excitation of S_1 and S_2 states with the corresponding resonant frequencies does not produce molecule bond breaking in the bis (2-ethylhexyl)-phthalate molecule, but could induce conformational changes which may disturb the PET polymer structure (polyethylene terephthalate), where the bis (2-ethylhexyl)-phthalate molecule is used as an additive that increases the plasticity or fluidity of PET polymer.

References

- [1.] G. Sun, C. Fecko, R. B. Nicewonger, W. W. Webb, and T. P. Begley, *Org. Lett.*, 2006, **8**, 681–683.
- [2.] MOLPRO, version 2009.1, A package of ab initio H.-J. Werner, P. J. Knowles, R. Lindh, F. R. Manby, M. Schütz, P. Celani, T. Korona, A. Mitrushenkov, G. Rauhut, T. B. Adler, et al. see <http://www.molpro.net>.
- [3.] T. H. Dunning Jr and P. J. Hay, in *Modern Theoretical Chemistry*, ed. H. F. Schaefer III, Plenum, New York, 1976, vol. 3, pp. 1–28.
- [4.] S. Matsika, *J. Phys. Chem. A*, 2004, **108**, 7584–7590.
- [5.] E. Epifanovsky, K. Kowalski, P.-D. Fan, M. Valiev, S. Matsika and A. I. Krylov, *J. Phys. Chem. A*, 2008, **112**, 9983–9992.
- [6.] I. J. Palmer, I. N. Ragazos, F. Bernardi, M. Olivucci and M. A. Robb, *J. Am. Chem. Soc.*, 1993, **115**, 673–682.
- [7.] P. J. Knowles and H.-J. Werner, *Theor. Chim. Acta*, 1992, **84**(1–2), 95–103.
- [8.] S. R. Langhoff and E. R. Davidson, *Int. J. Quantum Chem.*, 1974, **8**(1), 61–72.
- [9.] P. Celani and H.-J. Werner, *J. Chem. Phys.*, 2000, **112**(13), 5546–5557.
- [10.] H. J. Monkhorst, *Int. J. Quantum Chem.*, 1977, **12**(S11), 421–432.
- [11.] J. F. Stanton and R. J. Bartlett, *J. Chem. Phys.*, 1993, **98**(9), 7029–7039.
- [12.] T. Korona and H.-J. Werner, *J. Chem. Phys.*, 2003, **118**(7), 3006–3019.
- [13.] H. Eshuis, G. G. Balint-Kurti, F. R. Manby, *J. Chem. Phys.*, 2008, **128**, 114113.
- [14.] R. Peverati, and D. G. Truhlar, *J. Phys. Chem. Lett.*, 2012, **3**, 117–124.
- [15.] F. Weigend, R. Ahlrichs, *Phys. Chem. Chem. Phys.*, 2005, **7**, 3297–3305.

- [16.] W. H. Fang, D. L. Phillips, *ChemPhysChem*, 2002, **3**(10), 889–892.
- [17.] J. Li, F. Zhang, W. H. Fang, *J. Phys. Chem. A*, 2005, **109**(34), 7718–7724.
- [18.] Q. Fang, Y. J. Liu, *J. Phys. Chem. A*, 2010, **114**(1), 680–684.
- [19.] E. Runge, E. K. U. Gross, *Phys. Rev. Lett.*, 1984, **52**, 997.
- [20.] Y. Zhao, D. G. Truhlar, *Theor. Chem. Acc.*, 2008, **120**, 215.
- [21.] A. Schaefer, C. Huber, R. Ahlrichs, *J. Chem. Phys.*, 1994, **100**, 5829.
- [22.] Gaussian 09, Revision D.01, M. J. Frisch, G. W. Trucks, H. B. Schlegel, G. E. Scuseria, M. A. Robb, J. R. Cheeseman, G. Scalmani, V. Barone, B. Mennucci, G. A. Petersson, H. Nakatsuji, M. Caricato, X. Li, H. P. Hratchian, A. F. Izmaylov, J. Bloino, G. Zheng, J. L. Sonnenberg, M. Hada, M. Ehara, K. Toyota, R. Fukuda, J. Hasegawa, M. Ishida, T. Nakajima, Y. Honda, O. Kitao, H. Nakai, T. Vreven, J. A. Montgomery, Jr., J. E. Peralta, F. Ogliaro, M. Bearpark, J. J. Heyd, E. Brothers, K. N. Kudin, V. N. Staroverov, T. Keith, R. Kobayashi, J. Normand, K. Raghavachari, A. Rendell, J. C. Burant, S. S. Iyengar, J. Tomasi, M. Cossi, N. Rega, J. M. Millam, M. Klene, J. E. Knox, J. B. Cross, V. Bakken, C. Adamo, J. Jaramillo, R. Gomperts, R. E. Stratmann, O. Yazyev, A. J. Austin, R. Cammi, C. Pomelli, J. W. Ochterski, R. L. Martin, K. Morokuma, V. G. Zakrzewski, G. A. Voth, P. Salvador, J. J. Dannenberg, S. Dapprich, A. D. Daniels, O. Farkas, J. B. Foresman, J. V. Ortiz, J. Cioslowski, and D. J. Fox, Gaussian, Inc., Wallingford CT, 2010.